Article

Mummified fruits of *Canarium* from the upper Pleistocene of South China

Canarium maomingense sp. nov.

from the upper Pleistocene, South China

5 mm

5 mm

5 mm

Fungal fruiting body

300μm

5 mm

5 mm

Helanlin Xiang,
Tatiana M. Kodrul,
Mikhail S.
Romanov, ...,
Luliang Huang,
Xinkai Wu, Jianhua
Jin

kakukaikai@163.com (X.W.)
lssjjh@mail.sysu.edu.cn (J.J.)

Highlights

Canarium maomingense
sp. nov. described from
the upper Pleistocene of
South China

Micro-CT shows ovule
abortion in *Canarium*
existed at least since the
late Pleistocene

Fossil assemblage
suggests subtropical
evergreen broad-leaved
and mixed forests

Damage traces indicate
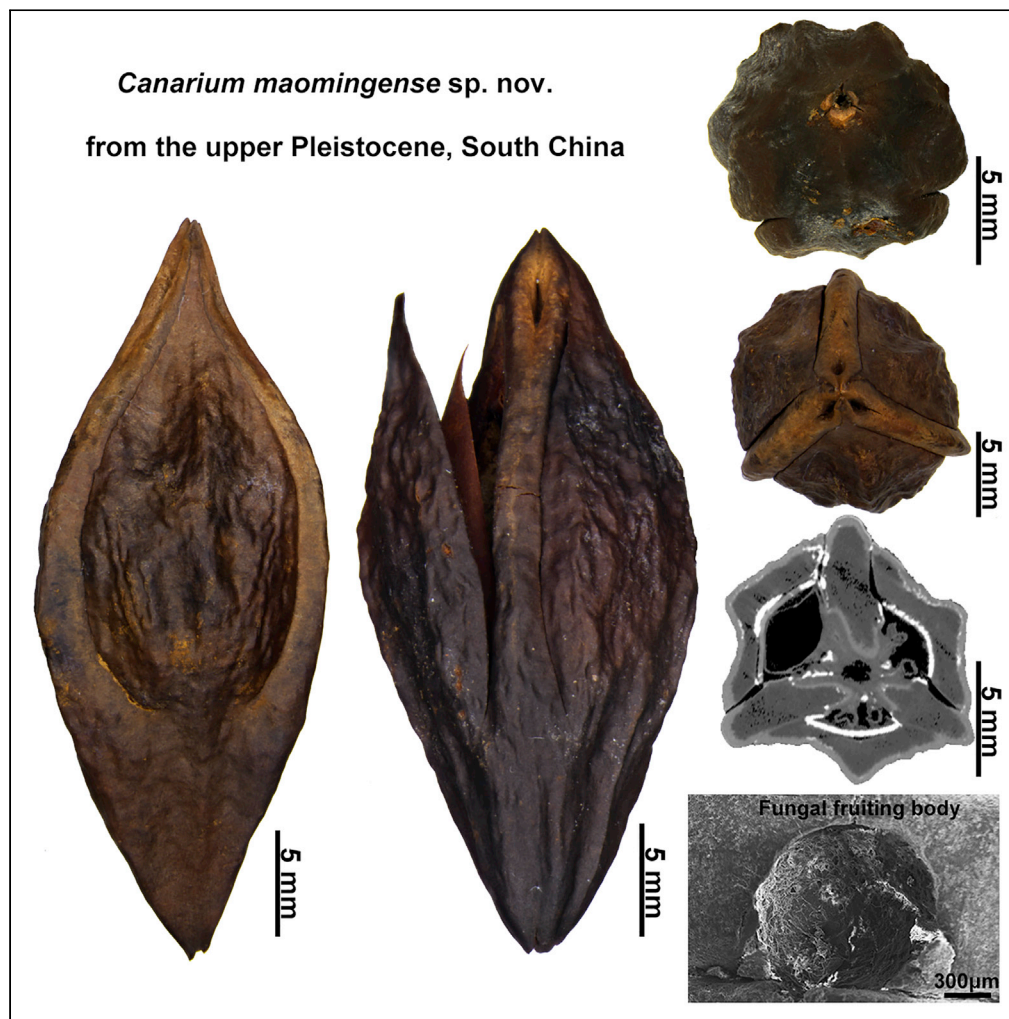possible interaction
among plants, animals,
and fungi

iScience

Article

Mummified fruits of *Canarium* from the upper Pleistocene of South China

Helanlin Xiang,[1] Tatiana M. Kodrul,[2] Mikhail S. Romanov,[3] Natalia P. Maslova,[4] Meng Han,[5] Luliang Huang,[6] Xinkai Wu,[6,7,*] and Jianhua Jin[1,*]

SUMMARY

***Canarium* L. contains approximately 78 species distributed in low to middle altitudes of the Paleotropics and northern Australia. *Canarium* fruit fossils are known mainly from Paleogene to Neogene of North America, Africa, and Eurasia. Here, we described a new species *Canarium maomingense* sp. nov. from the upper Pleistocene of the Maoming Basin, Guangdong, South China. Similarly to extant *Canarium* species, each of three locules of *C. maomingense* possesses two ovules, but only one or two of six ovules develop into a seed, indicating that the ovules undeveloped into seeds in *Canarium* species have existed at least since the late Pleistocene. The natural habitats of extant relatives and associated fossil plants suggest subtropical evergreen broad-leaved and mixed forests in the late Pleistocene of this region. Some special damage traces are observed on pyrene surfaces, indicating possible plant interactions with animals and fungi.**

INTRODUCTION

The family Burseraceae comprises ca. 700 species in 18 genera[1] and is divided into three tribes: Canarieae, Protieae, and Bursereae.[1–3] *Canarium* is the largest genus of the tribe Canarieae.[4] It contains ca. 78 species that are mainly medium- to large-sized canopy trees, distributed in low- to middle-altitude areas of the Paleotropics and northern Australia.[5,6] Seven *Canarium* species are native to the subtropical and tropical regions of southern China.[7] Formally, the fruit of *Canarium* is a syncarpous pyrenarium of the *Butia* type with a trilocular pyrene composed of an inner mesocarp zone and the endocarp. Each pyrene locule contains two hanging campilotropous ovules.[8–11] When the fruit matures, its peripheral soft tissues are eaten by animals or rot, and thus the hard pyrene is released. During seed germination, the pyrence surface cracks along distinct grooves bordering the lid (the germination valve) along the angle-ribs and the lid is pushed out from the inside by the growing seedling.

Currently known fossil remains of *Canarium* are represented by leaves, fruits, pollen, and wood.[12] The fossil fruits have mainly been recorded from the lower and middle Eocene of North America,[13,14] the middle Eocene of Europe,[15] the Oligocene of Asia, Europe, and Africa,[12,16–18] and the Miocene of Asia.[12,19,20] Leenhouts[5] supposed that the East Malaysian–northern Australia region was the most probable center of origin of *Canarium*, whereas analysis of the fossil records of this genus and its extant distribution suggests that *Canarium* originated in North America in early Eocene and migrated eastward to Europe during the middle Eocene.[1,12]

Canarium is an economically important plant having medicinal and food uses and hence has a long history of cultivation and consumption in Guangdong Province, other provinces of China and in some South-East Asian countries. However, the fossil records of this genus have not been reported from Guangdong Province until now. Thus, the well-preserved mummified *Canarium* fossil fruits, which have been recently found in the upper Pleistocene of Maoming Basin (Figure 1), are the first megafossil record of this genus in Guangdong Province. Here, we provide a morphological, anatomical, and taxonomic study of these fossils and apply the approach of the nearest living relative (NLR) method to analyze the paleoclimate in the region. The research is aimed at revealing the phytogeographical and phylogenetic significance of the new fossil records of *Canarium,* as well as focusing on clarifying their probable interactions with animals and fungi.

[1]State Key Laboratory of Biocontrol & Guangdong Provincial Key Laboratory of Plant Resources, School of Life Sciences, Sun Yat-sen University, Guangzhou 510275, China

[2]Geological Institute, Russian Academy of Sciences, Moscow 119017, Russia

[3]N.V. Tsitsin Main Botanical Garden, RAS, Moscow 127276, Russia

[4]Borissiak Paleontological Institute, Russian Academy of Sciences, Moscow 117647, Russia

[5]Shenzhen Museum, Shenzhen 518027, China

[6]School of Ecology, Sun Yat-sen University, Guangzhou 510006, China

[7]Lead contact

*Correspondence:
kakukaikai@163.com (X.W.),
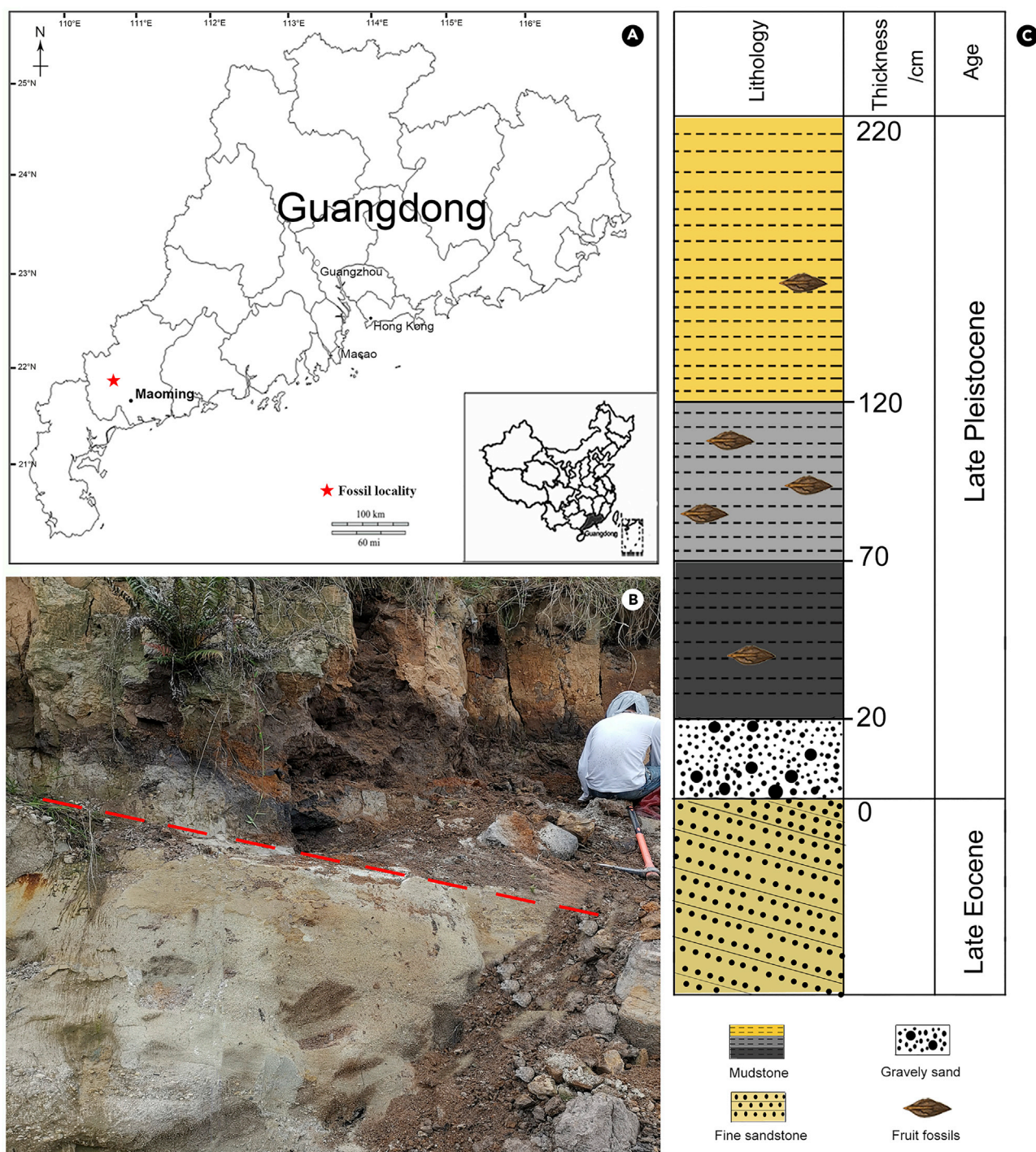lssjjh@mail.sysu.edu.cn (J.J.)

A

110°E 111°E 112°E 113°E 114°E 115°E 116°E

N

25°N

Guangdong

24°N

23°N   Guangzhou

Hong Kong

22°N   Macao

Maoming

21°N

★ Fossil locality

100 km
60 mi

B

C

Lithology | Thickness /cm | Age

220

120   Late Pleistocene

70

20

0   Late Eocene

Mudstone   Gravely sand

Fine sandstone   Fruit fossils

Figure 1. Location and lithology of the fossil site (modified from Huang et al.[21])

(A) Geographic map showing the location of the Zhenjiang opencast mine within the Maoming Basin in Guangdong Province, South China (base map from d-maps: https://d-maps.com).

(B) View of the plant-bearing section. Red dashed line indicates the unconformity between the upper Pleistocene deposits and the upper Eocene Huangniuling Formation.

(C) Lithological column of the studied succession showing the position of the *Canarium* fossil fruits.

RESULTS

Systematic paleontology

Order

Sapindales Juss. ex Bercht. et J. Presl (1820).

Family

Burseraceae Kunth (1824).

Genus

Canarium Linnaeus (1759).

Species

C. maomingense H.-L.-L. Xiang et J.-H. Jin sp. nov. (Figure 3A–3J, 4A–4G, 4J, 4K, 4L, 4O, 5, 8–10).

Etymology

The specific epithet ''*maomingense*'' refers to the Maoming Basin from where the specimens were collected.

Holotype

MMRH–192 (Figure 3A–3D, 4J, 4K, and 4O).

Specimens examined

MMRH–192; MMRH–193; MMRH–194; MMRH–195; MMRH–196; MMRH–197; MMRH–198; MMRH–207; MMRH–208; MMRH–209; MMRH–210; MMRH–211; MMRH–212; MMRH–213; MMRH–245; MMRH–246; MMRH–247 (total of 17).

Locality and age

Opencast mine near Zhenjiang Town, Maoming City, Guangdong Province; late Pleistocene.

Repository

The Museum of Biology of Sun Yat-sen University, Guangzhou, China.

Diagnosis

Pyrene spindle- to ovoid-shaped, with acute to attenuate apex and acute base, rounded (to hexagonal) in cross-section, trilocular, with two ovules per locule. Each locule with an outwardly projecting germination valve (lid), triangular at the top, with undulated or smooth surface and notably convex or slightly convex median longitudinal keel; all lids bordered along the angle-ribs by distinct grooves. Each of three angle-ribs (the septas comprising the three-rib central column) with an opening near the pyrene apex—the entrance into the septal vascular bundle channel. Pyrene wall composed of a thick mesocarp inner zone and the endocarp. The mesocarp inner zone consists of numerous layers of sclerenchyma and single innermost layer of thin-walled cells; the endocarp composed by single layer of obliquely radially elongated cells with wavy walls. Seeds one or two, the locules lacking the seed slightly undeveloped.

Description

The mummified fossils represent the pyrenes of syncarpous trilocular drupaceous fruits (Figure 2). The pyrenes are 24.78–33.38 mm long (mean 27.74 mm) and 9.52–14.35 mm wide (mean 12.66 mm), spindle- (Figures 3A, 3E, and 3F) to ovoid-shaped (Figure 3G), rounded (Figures 3B, 3C, 3I, and 3J) to hexagonal (Figures 3D and 3H) in cross-section; the apex is acute to attenuate (Figures 3A, 3E, 3F, and 3G), the base is acute and marked by a small attachment scar (Figure 3H). The pyrenes have three locules separated by a three-ribbed central column (Figures 2, 3D, 3I, and 3J). Each locule of the ovary has two ovules and axial placentation (Figures 4E, 4F, 4G, and 4L). Only one of the two ovules (or none) in each locule develops into a seed, and often only one per fruit, other ovules remain undeveloped into seeds (Figures 3D, 3I, 3J, 4J, 4K, and 4O). The locules with undeveloped seeds are slightly or significantly reduced
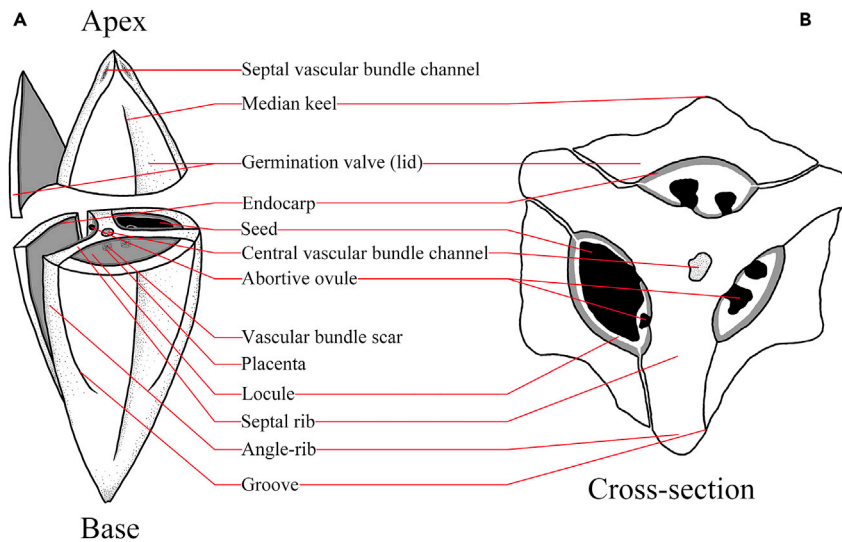
Figure 2. Morphology of a *Canarium* pyrene
(A) Side view and transverse section.
(B) Details of transverse section.

(Figures 3D, 3I, and 3J). The ovular vascular bundle scar is observed on the placenta (Figures 4G and 4L). Each locule has an outwardly projecting lid, triangular at the top (Figures 3A, 3E–3G, 4B, and 4D), which is 15.38–22.10 mm long (mean 17.95 mm), 6.58–10.73 mm wide (mean 9.34 mm), and 1.48–3.03 mm thick (mean 2.39 mm), it extends for 53.80%–73.37% of the pyrene length (mean 64.71%) (Figure 4B). The outer surface of the lids is undulated (Figures 3A, 3E, and 3F) or smooth (Figure 3G), with a median keel, which is notably convex (Figures 3A and 3E) or slightly convex (Figure 3G). The septal ribs between the locules are usually distinctly visible on the surface as the angle-ribs (Figures 3B–3D), which are 1.41–2.38 mm wide (mean 1.93 mm), and each of the three angle-ribs have a septal vascular bundle channel on the surface near the pyrene apex (Figures 3B, 3C, and 4J). The germination valves are bordered along the angle-ribs by distinct grooves. During germination, lids crack naturally along the grooves and become detached from the pyrene (Figure 3F). The seed coat (Figure 4A) and detached endocarp (Figures 4C–4F, 5C, and 5D) are observed in some specimens. The inner zone of the mesocarp is composed of numerous layers of mainly radially elongated sclerenchymatous cells with intercellular pits in the walls, which appear like dense hemispherical ornamentation (Figures 5A and 5B). These sclerenchymatous cells are rather polygonal in outline on the periphery of the pyrene and mainly isodiametric toward the inside (Figures 5A and 5B). The innermost zone of the mesocarp is represented by single layer of rather thin-walled cells (Figure 5E). Along this layer, which becomes relatively easily destroyed in fossil pyrenes, the endocarps can be separated from the hard mesocarp tissue (Figures 5C and 5D). The endocarp is composed by radially or obliquely radially elongated cells in relation to the center of the locule (Figures 5C–5F). The cells of the endocarp have thickened and considerably wavy walls with numerous pits and large pores, and are comparable with hydrocites in structure. The seed coats fuse with the perisperm and 1- to 2-layered endosperm, which contains idioblast cells visible on inner surfaces contacting the cotyledons (Figures 5C–5E).

DISCUSSION

Comparison of *C. maomingense* with extant species of *Canarium*

Fruits are considered to be conservative plant organs with a stable anatomical structure that is often used as an important taxonomic character. *Canarium* is distinguished from other genera in Burseraceae by its drupaceous fruit (pyrenarium) with three locules, and two hanging campilotropous ovules per locule.[1,6,7] Usually only one or two ovules (and in all cases only one per locule) develop into seeds.

Extant *Canarium* includes three taxonomic sections: *Canarium*, *Canariellum*, and *Pimela*.[5] The pyrenes of *C. maomingense* sufficiently differ from those of the sect. *Canarium* (pyrenes are usually 5–7 cm long,
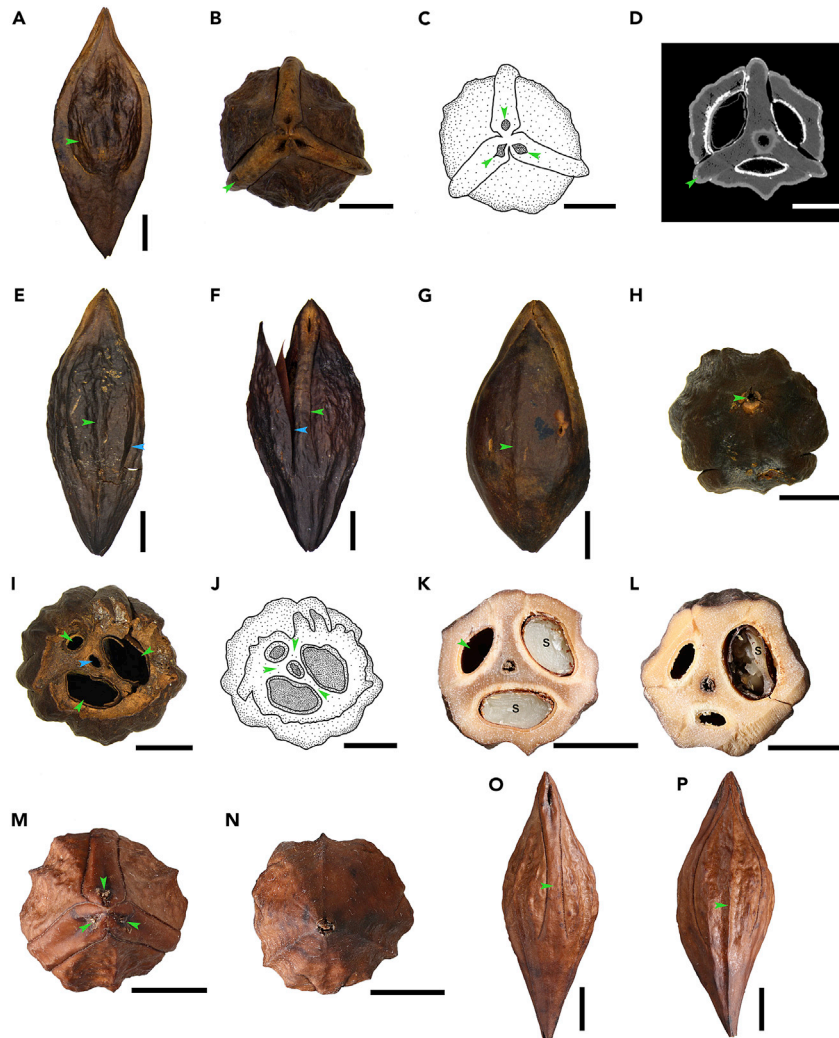
Figure 3. Pyrenes of fossil *Canarium maomingense* sp. nov. (A–J) and extant *Canarium album* (Lour.) Raeuschel (K–P)

(A) Lateral view showing the outwardly projecting lid (germination valve) with an undulated surface (arrow), holotype, MMRH–192. (B) Apical view of specimen in Figure 3A showing three angle-ribs that reflect the septal ribs between the locules (arrow). (C) Sketch of specimen in Figure 3B showing the septal vascular bundle channel (arrows). (D) Digital transverse section of specimen in Figure 3A showing the septal ribs between the locules and the angle-ribs (arrow), micro-CT. (E) Lateral view showing the median keel on the lid (green arrow) and distinct grooves between the angle-ribs and the lid (blue arrow), MMRH–193. (F) Lateral view of specimen in Figure 3E showing the lid that cracks along its outer boundary (blue arrow) and the groove (green arrow). (G) Lateral view showing the smooth lid with a slightly convex median keel (arrow), MMRH–196. (H) Base view showing the attachment scar and the entrance to the central vascular bundle channel (arrow), MMRH–197. (I) Transverse section showing the central vascular bundle channel (blue arrow) and three locules (green arrows), one of which is reduced, MMRH–211. (J) Sketch of fruit in Figure 3I showing the septal ribs (arrows).

(K) Almost circular transverse section showing two seeds (s) and one sterile locule (arrow). (L) Almost hexagonal transverse section showing a seed (s) and two undeveloped sterile locules. (M) Apical view, note the septal vascular bundle channels (arrows). (N) Base view. (O) Lateral view, note the angle-rib (arrow). (P) Lateral view, note the median keel of the lid (arrow). Scale bars = 5 mm.

smooth, sometimes with angle- and median ribs);[5] thus, we compared fossil pyrenes with those of the sections *Canariellum* and *Pimela* (Table S1). Pyrenes of the new fossil species are morphologically more similar with those of some extant *Canarium* species of sect. *Pimela* (*Canarium album* (Lour.) Raeuschel, *C. bengalense* Roxb., *C. tonkinense* Engl., *C. pimela* Leenh., *C. parvum* Leenh., *C. subulatum* Guillaumin, and *C. strictum* Roxb.).[5,7,12] Among these extant species, *C. album* (Figures 3K–3P, 4H, 4I, 4M, and 4N) is
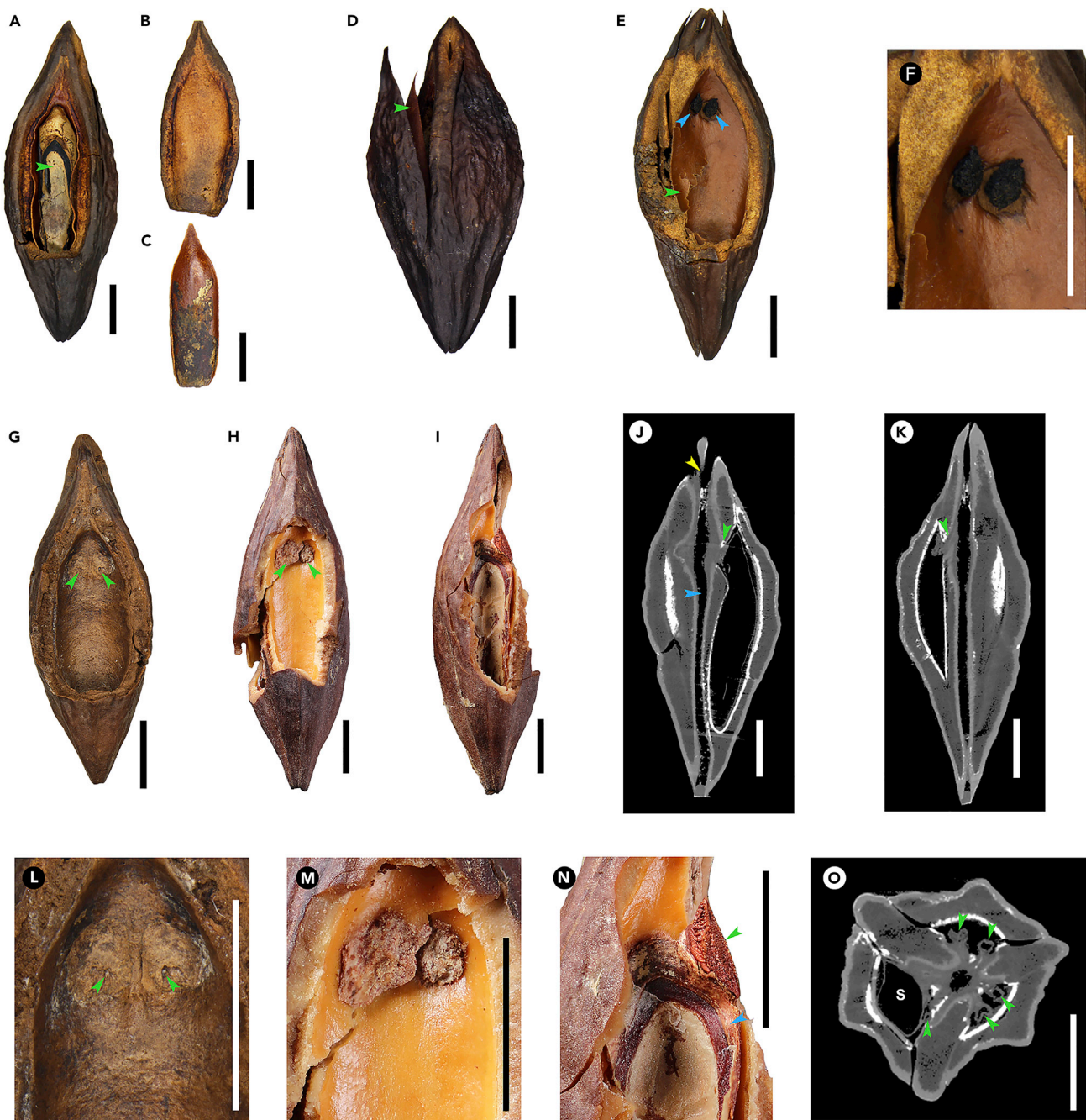
Figure 4. Internal structure of pyrenes of fossil *Canarium maomingense* sp. nov. (A–G, J–L, O) and extant *Canarium album* (Lour.) Raeuschel (H, I, M, and N)

(A–D) MMRH–193. (A) Lateral view showing the endosperm inner surface (arrow). (B) The lid, the locule-faced surface. (C) Exfoliated endocarp. (D) Lateral view showing the endocarp (arrow).

(E) Lateral view showing the endocarp lining the locule (green arrow) and two placentas (blue arrows), MMRH–197.

(F) Enlarged view of two placentas in Figure 4E.

(G) Lateral view showing two placentas and ovular vascular bundle scars (arrows) (MMRH–213).

(H) Lateral view showing two placentas (arrows).

(I) Lateral view showing the endosperm inner surface.

(J) Longitudinal section showing the central vascular bundle channel (blue arrow), which merges at the top with the septal vascular bundle channel (yellow arrow), and the attachment of a normally developed ovule/seed (green arrow), holotype, MMRH–192, micro-CT.

Figure 4. Continued

(K) Longitudinal section showing the central vascular bundle channel and the point of attachment of an aborted ovule (arrow), holotype, MMRH–192, micro-CT.

(L) Enlarged view of two placentas in Figure 4G showing ovular vascular bundle scars (arrows).

(M) Enlarged view of two placentas in Figure 4H.

(N) Enlarged view of the endosperm inner surface (blue arrow) and undeveloped seed (green arrow) in Figure 4I. (O) Transverse section showing the attachment and development of the aborted ovules in the locules (arrows), next to a normally developed locule with a seed (s), holotype, MMRH–192, micro-CT. Scale bars = 5 mm.

most similar to the new fossil species in terms of the pyrene shape (spindle to ovoidal) and proportions as well as in anatomical features. The mean thickness of the lid in *C. maomingense* and *C. album* is basically the same. However, the diameter of the *C. maomingense* pyrene (9.52–14.35 mm) is smaller than in *C. album* (15–20 mm), and some of the studied fossil specimens have a smooth lid and median keel that is markedly convex, but the lid of extant *C. album* is undulated, and its median keel is slightly convex. The inner mesocarp sclereids that compose the outer part of the pyrenes are smaller and more isodiametric in extant species (50–90 × 20–30 μm in *C. album* vs. 80–140 × 20–30 μm in *C. maomingense*), and the endocarp thickness in *C. album* (up to 200–220 μm) noticeably exceeds that in the fossil species (70–90 μm) (Figures 6A, 6B, 6E, and 6F). The innermost layer of the mesocarp in *C. album* consists of thin-walled cells that are mostly flattened in a radial direction and contain dense substances of an unknown nature in the lumina with bagel-shaped outlines (Figure 6D). Along this thin-walled cell layer (Figures 6C and 6D), the separation of the sclerenchymatous inner mesocarp zone and the endocarp occurs in dehiscent and partly decayed pyrenes, and the endocarps that are occasionally fused with seed coats, perisperm, and endosperm exfoliate out of the locule in *Canarium* species.

The new fossil species is also similar to *C. bengalense* in the shape of the pyrene cross-section and the thickness of the lid. However, both the length (24.78–33.38 mm) and width (9.52–14.35 mm) of the studied fossil specimens are smaller in comparison with those of *C. bengalense* (length 45–50 mm, width 17.5–20 mm). The large pyrene of the fruit of *C. bengalense* is spindle shaped with a triangular to circular cross-section; the smooth lid has unobvious median keel. The angle-ribs of *C. bengalense* often protrude over the pyrene surface up to 5 mm.

The pyrenes of *C. maomingense* and *C. tonkinense* are similar in having an undulated to smooth lid. However, the lid median keel in the fossil species generally protrudes markedly from the surface, whereas in *C. tonkinense* the keel is not seen. Nevertheless, in *C. tonkinense*, the pyrenes are ellipsoidal in shape, with obtuse apices and bases, and are circular-triangular in cross-section, unlike in the Maoming fossils. The pyrene diameter (on average 12.7 mm) in *C. maomingense* is smaller than that in *C. tonkinense*.

Pyrenes of the new fossil species differ from those of *C. pimela*, which have a narrowly ovoidal shape, a nearly circular cross-section with a diameter of 17.5–20 mm, a smooth lid surface (3 mm thick), and an inconspicuous lid median keel.

In contrast to *C. maomingense*, pyrenes of *C. parvum* are spindle shaped with thin lids (1 mm vs. 1.48–3.03 mm in *C. maomingense*). In addition, the surfaces of *C. parvum* lids are smooth with obscure median keels, and the cross-sections are triangular, differing from the Maoming fossils.

The pyrene of *C. subulatum* is oval in outline, the lid surface is smooth with an obscure median keel, and the cross-section is circular-triangular, up to 15–20 mm in diameter, and so differing from the much smaller rounded-hexagonal cross-sections of the pyrenes of *C. maomingense*.

The pyrene lengths and diameters of *C. maomingense* are smaller than those of *C. strictum* (32.5–45 mm long and 17.5–22.5 mm wide), and the pyrene shape of the extant species is obovoid to ellipsoid, nearly circular to rounded triangular in cross-section, and blunt at the base and apex. The lid median keel of pyrenes of the Maoming fossil species and *C. strictum* are prominent or obscure, but the lid surface of the fossil specimens is smooth to undulated, whereas in *C. strictum* it is smooth.

Thus, the *Canarium* fossil fruit pyrenes studied in this paper are different in various ways from the extant Chinese and South-East Asian species mentioned above, and cannot be assigned to anyone of them.
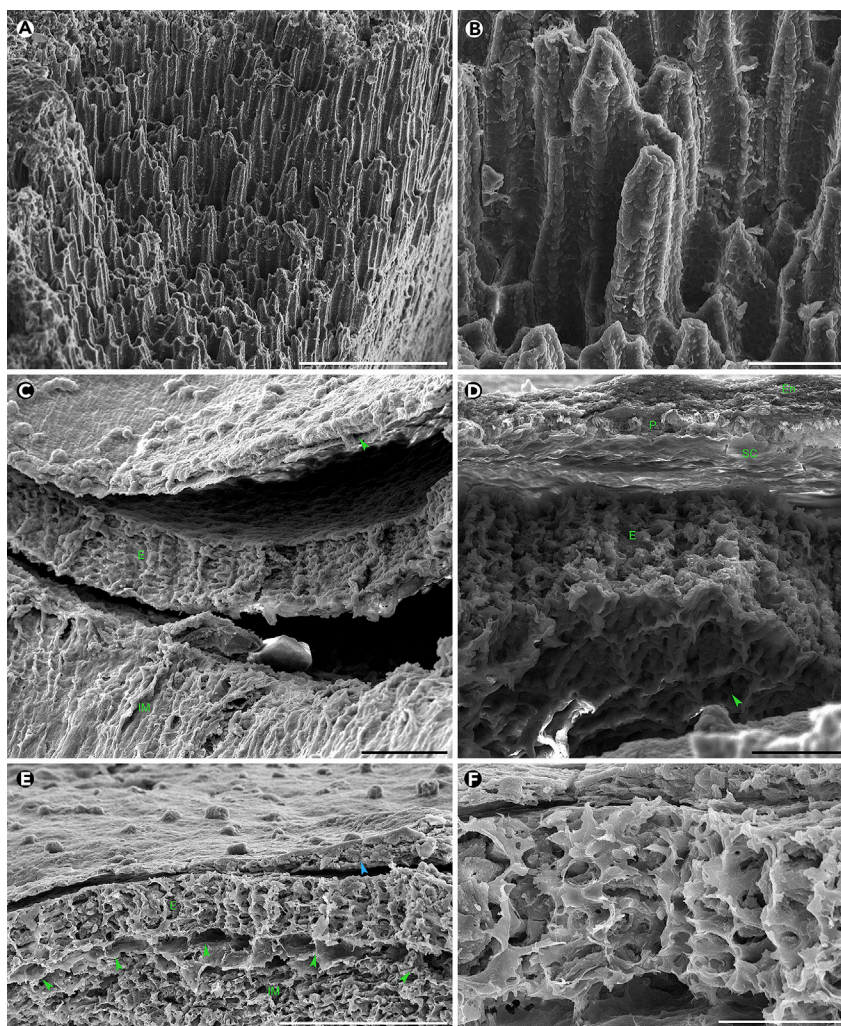
Figure 5. Fruit anatomy of fossil *Canarium maomingense* sp. nov., MMRH–196, SEM

(A) Radially elongated sclerenchymatous cells of the pyrene inner mesocarp.

(B) Enlarged view of mesocarp sclerenchymatous cells with intercellular pits in the walls, which appear like dense hemispherical ornamentations of the cell walls.

(C) Mainly isodiametric cells of the inner part of hard mesocarp tissue (IM), detached endocarp (E) composed of radially elongated cells with thickened wavy walls, and the seed coat fused to the perisperm and endosperm that contains idioblast cells (arrow).

(D) Detached endocarp (E) and seed coat (SC) fused with the perisperm (P) and endosperm (En). Note the outer surface of the endocarp (arrow).

(E) Inner part of hard mesocarp tissue (IM), endocarp (E) composed of a single layer of elongated cells, and the seed coat fused with the perisperm and endosperm containing idioblasts (blue arrow). Note the innermost layer of mesocarp consisting of thin-walled cells (green arrows).

(F) The endocarp composed of elongated cells with thickened wavy walls having numerous pits and large pores. Scale bars: (A) = 300 μm; (E) = 200 μm; (C) = 100 μm; (B, D, F) = 50 μm.

Comparison of *C. maomingense* with fossil representatives of Burseraceae

Several extinct taxa are supposed to be closely related to *Canarium* (Table S2). One of them is *Tricarpellites communis* Bowerbank from the lower Eocene London Clay Formation, United Kingdom.[22] *C. maomingense* is similar to *T. communis* in having syncarpous fruits with three locules along the main axis and axial placentation. However, the pyrenes of *T. communis* are sub-ovoid in shape, triangular in cross-section, and with a smooth lid surface. The lengths and widths of the pyrenes, and the widths of the lids (6.58–10.73 mm) of the Maoming specimens are
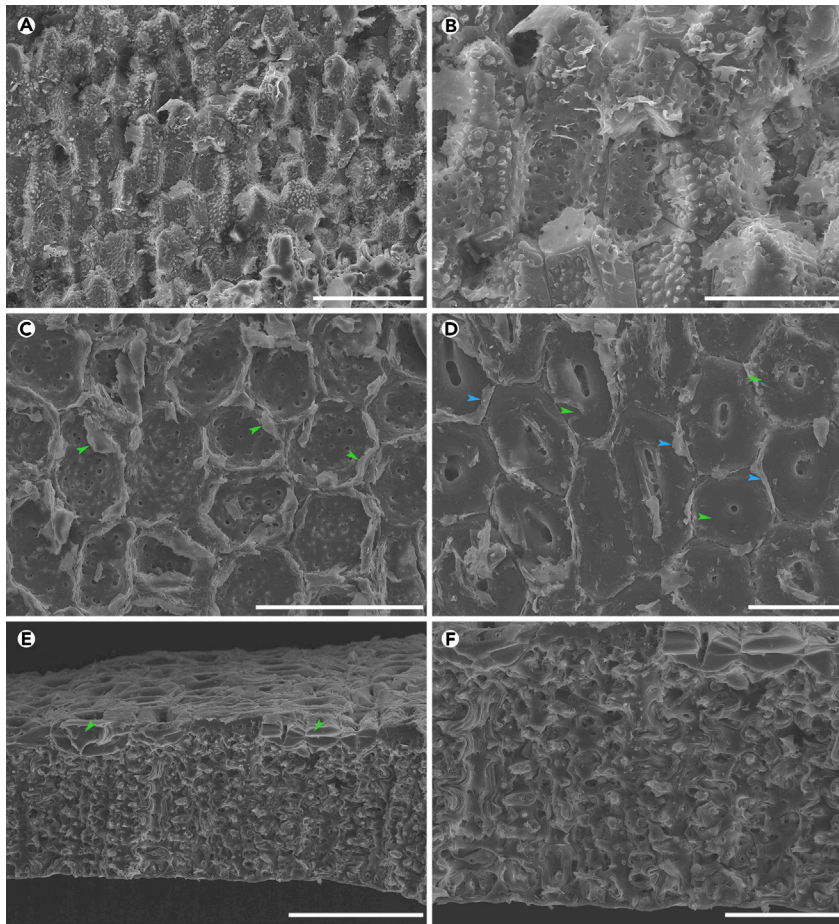
Figure 6. Pyrene anatomy of extant *Canarium album* (Lour.) Raeuschel, SEM

(A) Elongated sclerenchymatous cells of the pyrene inner mesocarp.

(B) Enlarged view of the mesocarp sclerenchymatous cells with intercellular pits in the walls.

(C) Inner view of the surface of the inner sclerenchymatous zone of the mesocarp. Note the broken walls of the cells of the mesocarp innermost layer along which the pyrene is fractured (arrows).

(D) Outer surface view of the exfoliated inner part of the pyrene showing the cells of the innermost layer of the mesocarp containing dense substances in the lumina with bagel-shaped outlines (green arrows). Note the broken thin cell walls (blue arrows).

(E) The endocarp composed of a single layer of elongated cells and the innermost thin-walled cell layer of the mesocarp (arrows).

(F) The endocarp cells with thickened wavy walls. Scale bars: (C and E) = 200 μm; (A, D, and F) = 100 μm; (B) = 50 μm.

larger than those of *T. communis* (7.5–12.5 mm × 4.25–7.5 mm in size, with 4.25–4.5 mm lid width). The lid length in *C. maomingense* is about 2/3 of the length of the pyrene, whereas in *T. communis* it is about 1/3 to 1/2 of the pyrene length. The specimens from the London Clay have tendency to split into separate pyrenes, possibly, the consequence of partial decay before fossilization.[22]

Agarwal and Ambwani[23] described carbonaceous angiosperm fruit fossils from the Miocene of Sindhudurg District, Maharashtra, India. The detailed morphological characteristics of these fruits, which they assigned to the species *Canariocarpon ratnagiriensis* Agarwal et Ambwani, indicate that they are related to the genus *Canarium*. The Maoming and Indian species are similar in the shape of their trilocular pyrenes; however, those of *C. ratnagiriensis* are larger (about 30–45 mm long and 13–20 mm wide), and the width of the lid is 7–20 mm. Moreover, some of our specimens have prominent median keels, whereas the median keels of *C. ratnagiriensis* are not prominent.

Pyrenes of *Canarium parksii* Tiffney from the lower Eocene of Virginia, USA[13] were recently scanned with micro-CT.[12] *C. maomingense* and *C. parksii* differ in their complex of characters. The pyrenes of *C. parksii* are much smaller (5.8–9.0 mm long and 2.5–5.6 mm wide), teardrop shaped, triangular in cross-section, and with an indistinct median keel on a smooth lid surface. Moreover, the point of vascular attachment in *C. parksii* is approximately in the middle of the seed length, whereas in *C. maomingense* it is located about 1/5 of the seed length from its apex.

Canarium sp. from the middle Eocene Wagon Bed Formation of Wyoming, USA[14] is comparable to *C. maomingense* in size being 27 mm long. However, the fossil specimen from Wyoming is preserved as a silica cast, lacking anatomical details for further comparison.[12]

Unlike in the species described here, pyrenes of *Canarium* sp. from the middle Eocene Messel Formation, Germany[15] are elliptical to oval in lateral view, with obtuse apices and bases, 12 mm long and 8 mm wide, triangular in cross-section, and with quite narrow grooves between the angle-ribs and smooth lids.

Pyrenes of *C. maomingense* are close in size to those of *Canarium chandleri* Gregor et Goth (18–28 mm long, 13–15 mm in diameter) from the Oligocene of the Czech Republic.[16] However, pyrenes of *C. chandleri* are nearly oval in lateral view, with a triangular cross-section and lids that extend for about 3/4 of the total pyrene length, in contrast to about 2/3 in *C. maomingense*.

Recently, two fossil species of *Canarium* were described from South and East China. Han et al.[12] reported the *Canarium guangxiense* Han et Manchester from the Yongning Formation (upper Oligocene) of Nanning City, the Erzitang Formation (Miocene) of Guiping City and the Foluo Formation (upper Miocene) of Beihai City, Guangxi Province. The original spelling of a specific epithet *guangxiensis* is modified here to correct the terminal ending of the specific epithet according to the grammatical gender of the generic name *Canarium* (*lat.* Neutrum) in conformity with Art. 23 of the International Code of Nomenclature for algae, fungi, and plants.[24] The pyrenes of *C. maomingense* and *C. guangxiense* are similar in size and shape, although pyrenes of *C. guangxiense* often tend to be obovoid with an attenuate apex. In contrast to *C. maomingense*, the pyrenes of *C. guangxiense* are three- and four-locular, sometimes with triangular cross-sections. The pyrenes of *C. maomingense* are more elongated (length/width ratio 2.7 in average) as compared with those of *C. guangxiense* (length/width ratio 2.4 in average). Furthermore, in *C. maomingense*, the lid extends up to 2/3 of the pyrene length, whereas in *C. guangxiense* it reaches 4/5 of the pyrene length.

Canarium haominiae Yin, Wu, Wang et Shi from the middle Miocene Fotan Group in Fujian Province, China, distinctly differs from *C. maomingense* in having mainly ovoid (in lateral view) pyrenes, rounded triangular in cross-section, with acute to obtuse bases and slightly acuminate to acute apices and pyrene length/width ratios of about 1.6–2.2 (commonly 1.8).[20]

Hence, the comparison of morphological characteristics displayed by the fruit fossils from the Maoming Basin studied in this paper shows that they differ from those of previously described fossil species and therefore we assign our fossils to a new species.

Paleophytogeographical and paleoecological implications

Based on the modern distribution of the Burseraceae in the American, African, and Indo-Asian tropics, and their highest generic diversity being in the Southern Hemisphere, Leenhouts[5] and Raven and Axelrod[25] considered that this family may have originated in tropical Gondwana and experienced vicariance as a result of Gondwanan fragmentation. McLaughlin[26] suggested that the vicariance of Gondwanan angiosperms may be associated with more recent tectonic events, such as the collision of the Indian subcontinent with Asia followed by angiosperm dispersal to other regions of Northern and Southern Hemispheres. Lam[27] also presumed that some genera of Burseraceae, in particular, *Canarium* may have originated in Africa and then reached Asia via the India connection. However, the estimates of divergence time for a number of tropical angiosperm lineages have indicated that Northern Hemisphere land connections had more influenced on the plant migration than previously hypothesized.[1,28–30] Based on nuclear and chloroplast sequence data and fossil calibration of the molecular phylogeny, Weeks et al.[1,30] suggested a North American origin of Burseraceae in the Late Cretaceous followed by migration of its lineages eastward over the North Atlantic land bridge to Europe and along
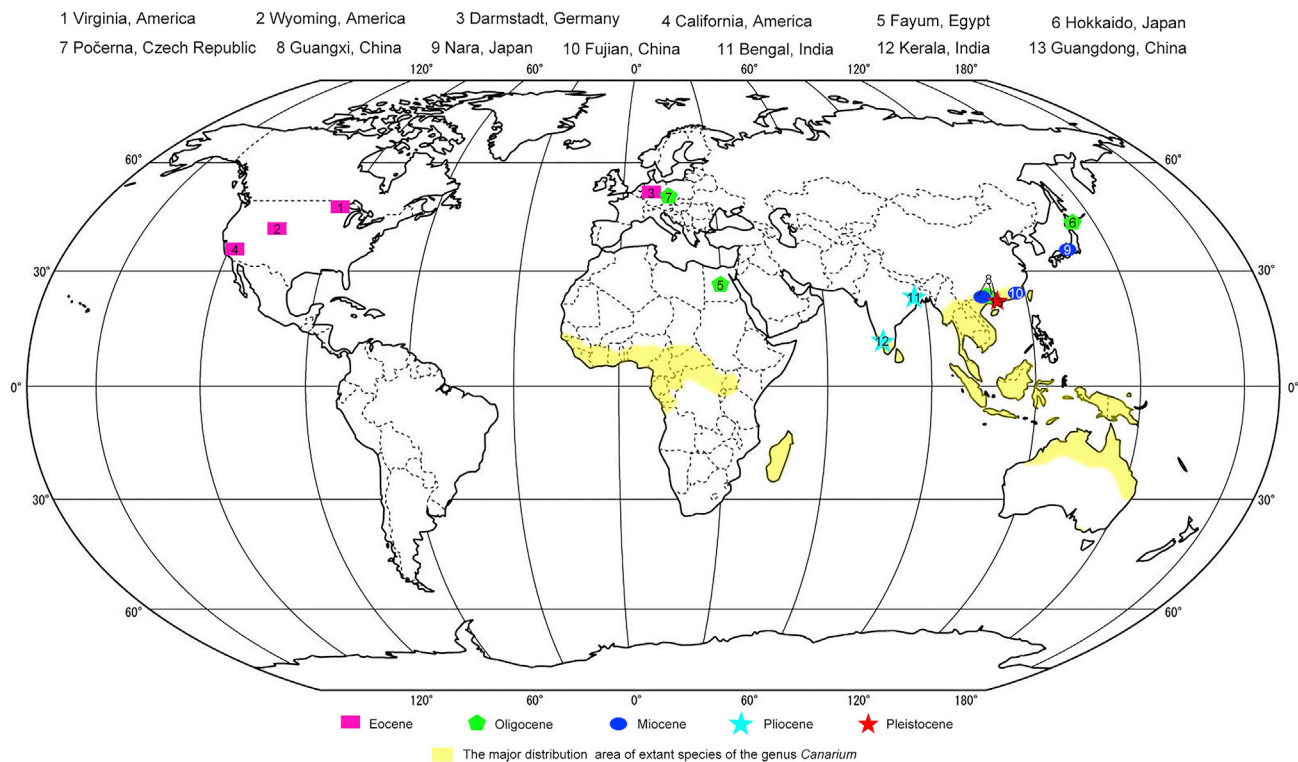
Figure 7. Megafossil records of *Canarium* (Table S3) and the major native ranges of its extant species

The extant species ranges of *Canarium* are from Global Biodiversity Information Facility (GBIF.org (24 July 2022) GBIF Occurrence Download https://doi.org/10.15468/dl.6nhprp).

the northern margin of Tethys Sea to Southeast Asia, as well as long distance dispersals to Africa and South America.

Although fossil records of *Canarium* are scarce, their occurrences known to date are consistent, generally, with the Burseraceae diversification history proposed by Weeks et al.[1,30] The oldest fruit fossils of *Canarium* come from the lower Eocene of western North America (Figure 7). By the middle Eocene, the genus extended throughout North America and had entered Europe. In the Oligocene, the reconstructed climate in most of Eurasia resembled that of a subtropical humid climate with distinctive seasonality,[31,32] and frost-intolerant *Canarium* spreads across Europe, Asia, and northern Africa. During the Miocene, populations of *Canarium* from high- and mid-latitude regions of the Northern Hemisphere were presumably eliminated during global climate cooling at the Oligocene-Miocene transition[33,34] and were forced to move southward into more favorable climates. The Miocene occurrences of *Canarium* are currently known only from southern Japan and southern China, while Mio-Pliocene *Canarium* fossils are restricted to India (Figure 7). For the Pleistocene and Holocene, *Canarium* is limited to southern Asia, Africa, northern Australia, and the Pacific Islands, which corresponds with the extant range of the genus.[35–37]

Canarium first appears in South China in the late Oligocene and becomes more diverse in the Miocene. Pyrenes of both species from Guangxi and Guangdong provinces, previously described as the late Oligocene-Miocene *C. guangxiense*[12] and the newly recognized late Pleistocene *C. maomingense*, morphologically closely resemble those of the extant *C. album*. Moreover, two pyrenes from the Miocene of Japan[19] were assigned to the extant *C. album*. Hence, the fossil species related to *C. album* existed within a region close to the modern native range of this extant species from at least the late Oligocene.

C. album is native to the subtropical and tropical regions of southern China (Yunnan, Guangxi, Guangdong, Fujian, and Taiwan) and Vietnam approximately between 22°N and 26°N.[7,38] Evergreen trees of this species

are distributed mainly in primary and secondary forests in valleys and on hillsides below 1300 m above sea level. Like all other members of Burseraceae, *C. album* is cold sensitive and thrives at an annual average temperature of 22°C–23°C, with an annual rainfall of above 1500 mm.[39,40] However, the species can withstand temperatures below 6°C–7°C in the winter as well as long periods of drought in the summer, with temperatures of about 40°C.[41] According to the NLR method, we assume that the new fossil species from the Maoming Basin possessed similar paleoclimatic and paleoecologic growing conditions. The fossil plant assemblage associated with *C. maomingense* at the locality includes identified to date conifers of the genera *Pinus* and *Keteleeria* (Pinaceae) and angiosperms belonging to *Elaeocarpus* (Elaeocarpaceae), *Liquidambar formosana* Hance (Altingiaceae), and Fagaceae.[21,42,43] Most of these taxa occur in the modern subtropical evergreen broad-leaved and mixed forests of Eastern Asia.[38,44] Based on growth ring analysis of fossil wood of *Keteleeria* sp. and *L. formosana*, and that of extant species *Keteleeria davidiana* (C.E. Bertrand) Beissn., a monsoon-influenced humid subtropical climate with hot wet summers and cool dry winters was interpreted for the Maoming Basin region during late Pleistocene.[21,42] These conditions are similar to the humid subtropical climate classified as Cwa, under the Köppen climate classification,[45,46] that prevails at present in northeastern Vietnam.

Canarium fossil records reported from the upper Oligocene of Nanning, the Miocene of Guiping and the upper Miocene of Beihai, Guangxi,[12] as well as the upper Pleistocene of Maoming, Guangdong, all fall within the modern distribution range of this genus. It can be speculated that, in the gradually intensifying Cenozoic global cooling, *Canarium* may have continued to exist in this region since the late Oligocene. In the past 66 Ma, four Earth's climate states are identified based of their response to astronomical forcing depending on greenhouse gas concentrations and polar ice sheet volume: Warmhouse (66–56 Ma and 47–34 Ma), Hothouse (56–47 Ma), Coolhouse (34–3.3 Ma), and Icehouse (3.3–0 Ma).[34] The late Pleistocene *Canarium* from the Maoming Basin experienced Icehouse climate state, when the average temperature was generally lower than today. Even despite the fact that this fossil site is located near the northern border of the modern genus range (Figure 7), the late Pleistocene climate of this region was favorable for the survival of the frost-intolerant *Canarium*. It can be inferred from the genus distribution that the influence of Pleistocene Icehouse climate in southern China was limited.

Specific fruit characters of fossil and extant *Canarium* species

Extant *Canarium* fruits are trilocular with two hanging campilotropous ovules per locule, of which only one or rarely two locules contain a developed seed (Figure 3K and 3L), usually a single large seed with twisted cotyledons.[6,7] Placenta (Figures 4H and 4M), the position of the ovule attachment, can be seen on the endocarp, and normally the seeds or/and the ovule(s) which do not develop into the seed can be observed in locule (Figures 4I and 4N) in extant *Canarium*. The micro-CT and macro-observations of *C. maomingense* pyrenes have revealed two ovules per locule, but only one ovule per locule (or none) develops into a seed and others remain undeveloped (Figure 4O). The ovule is attached to the placenta (Figures 4E, 4F, 4G, and 4L) and connected with the ovular vascular bundle which branches from the central vascular bundle (Figures 4J, 4K, and 4O). These characteristics are identical with the extant *Canarium* species and indicate that this phenomenon of *Canarium* fruit development had existed in the late Pleistocene.

Relationships with other organisms

Weeks et al.[1] pointed out that the fruits of the Burseraceae do not have morphologies related to external and passive transmission by animals such as viscous mucus or hooks, but some genera have fruits more likely to be dispersed by animal feeding behavior. Animals either discard the inedible part of fruit immediately after eating the fleshy part of the pericarp or aril, or excrete some complete hard and stony parts after digestion. The fleshy and juicy mesocarp of *Canarium* fruits may attract animals, while some animals may destroy the pyrene in order to obtain nutritious seeds of *Canarium*.

Some damage can be seen on the surfaces of fossil pyrenes, such as dents (Figures 8A and 8B), scratches (Figures 8, 9C, 9D, and 9E), relatively small rounded or oval holes (Figures 9A, 9B, 10D, 10F, and 10H), holes of various shapes (Figures 9C and 9D), traces of surface biodegradation of uncertain nature (Figures 8B, 9E, 9F, 10A, and 10B), and evidence of fungal attack (Figures 9G, 10C, 10E, and 10G). There is a certain regularity in the scratch damage on some pyrene surfaces, and many of them are a group of three marks (Figures 8B, 8C, 8E, 8F, and 9C), which is obviously different from the random and irregular scratch that may be caused by water transportation and other
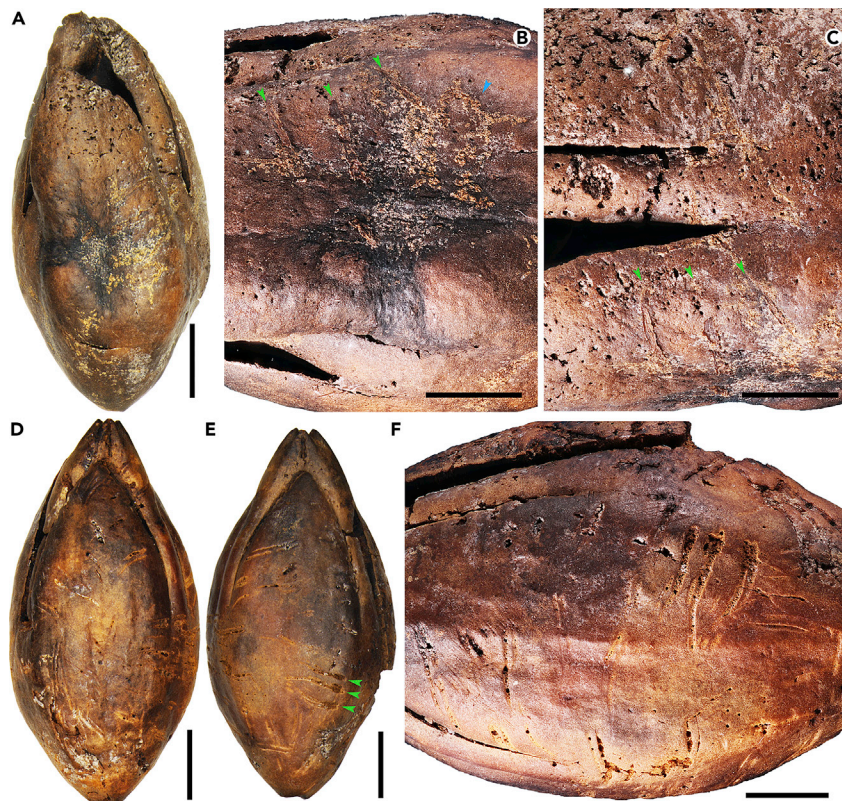
Figure 8. Damage on the pyrenes of *Canarium maomingense* sp. nov

(A) Pyrene with a dent and scratches, MMRH–209.

(B) Enlarged view of Figure 8A showing a dent (blue arrow) and group of three scratches (green arrows).

(C) Enlarged view of Figure 8A (underside of pyrene) showing a group of three scratches (arrows).

(D–E) Dense regular scratch marks, note a group of three scratches in (E) (arrows), MMRH–212.

(F) Enlarged view of Figure 8E showing a group of three scratches. Scale bars: (A, D, and E) = 5 mm; (B, C, and F) = 3 mm.

taphonomic processes. These damage types are probably caused by the teeth or claws of animals scraping the fleshy mesocarp. According to a range of studies, birds such as pigeons and hornbills as well as mammals of the order Chiroptera (e.g., bats and flying foxes), lemurs, squirrels, and terrestrial mammals such as rodents and deer consume the fleshy mesocarp and seeds of *Canarium* fruits.[47–51] Flying foxes (bats) are considered to be active consumers of *Canarium* fruits,[50] and originated in the early Pliocene and diversified during the Pleistocene inhabiting tropical regions of Asia, Australia, Africa, and some Pacific Islands.[51] A variety of dents and holes can be created by animals as a result of attempts to gnaw the hard pyrene in search of a nutritious seed inside. Larger holes of various shapes, accompanied by cracks of the pyrene wall, may have resulted from pyrene splitting by mammalian teeth (Figures 9C and 9D). Single small holes that appear in some pyrenes (Figures 9A, 9B, 10D, 10F, and 10H) are similar to the damage caused by insects like weevil beetles (family Curculionidae). Some weevil beetles, for example *Ectatorhinus magicus* Gerstaecker,[50] can lay their eggs in fruits by piercing fleshy tissue as well as the woody endocarps/shell of the fruit, and also feed on dying wood.[52]

Numerous different in size, shape, and depth superficial damage on the pyrenes are interpreted as a traces of surface biodegradation caused by unknown microorganisms (Figures 8B, 9E, 9F, 10A, and 10B). Such damage can be inflicted by bacteria or microscopic fungi whose metabolites initiate a set of plant tissue-destroying chemical and physical processes. A single fungal fruiting body was noted on the surface of *Canarium* pyrene (Figures 9B, 9G, 10C, and 10E). The fruiting body is immersed in the tissue of the plant host, rounded in shape, with a diameter of 1.2 mm. The ostiole is inconspicuous. Free hyphae occur on the surfaces of the endocarp and fruiting body (Figures 10E and 10G). This fruiting body can be compared to those of the genus *Coleophoma* Höhn. (Ascomycota) characterized by similar hemispherical pycnidia,
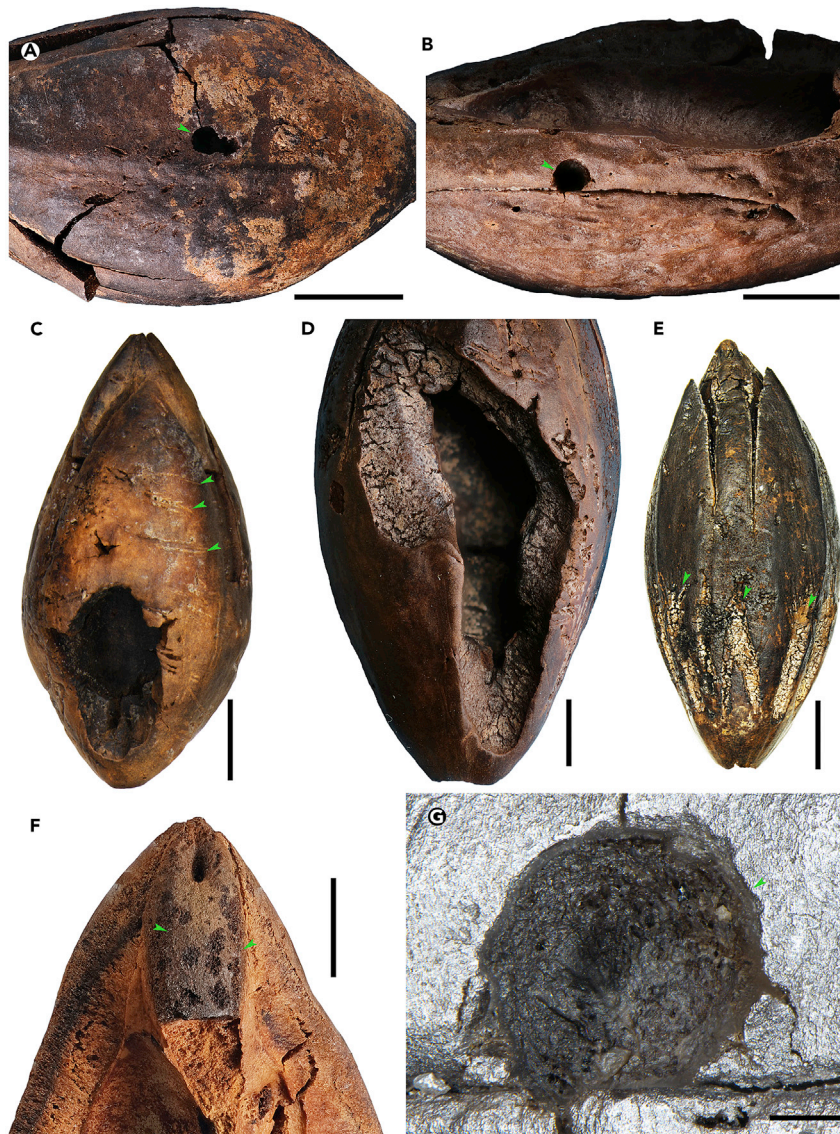
Figure 9. Damage on the pyrenes of *Canarium maomingense* sp. nov

(A) Round hole (arrow) accompanied by cracks, MMRH–210.

(B) Fungal fruiting body (arrow), MMRH–213.

(C) Oval hole and three scratches (arrows), MMRH–212.

(D) Hole and scratches, MMRH–246.

(E) Scratches with the traces of surface biodegradation (arrows), MMRH–246.

(F) Shallow superficial damage (arrows) of unknown nature, MMRH–196.

(G) Enlarged view of Figure 9B showing fungal fruiting body (arrow). Scale bars: (A and E) = 5 mm; (B–D and F) = 3 mm; (G) = 0.3 mm.

immersed in the host plant tissue, with a non-papillate inconspicuous ostiole. *Coleophoma* occurs on a wide range of plant hosts and includes species that are saprobic or plant pathogenic.[53] This fungal genus also has been identified on the fruits of extant *Canarium indicum* L.[50]

Consequently, the damage types described here indicate possible co-evolutionary relationships between plants and some mammals and/or birds. These frugivores could use *Canarium* fruits as a food source, as well as serve as seed dispersal agents for this plant. The type of relationships between *Canarium* and micro-scopic organisms (micromycetes and/or bacteria) is not yet well understood.
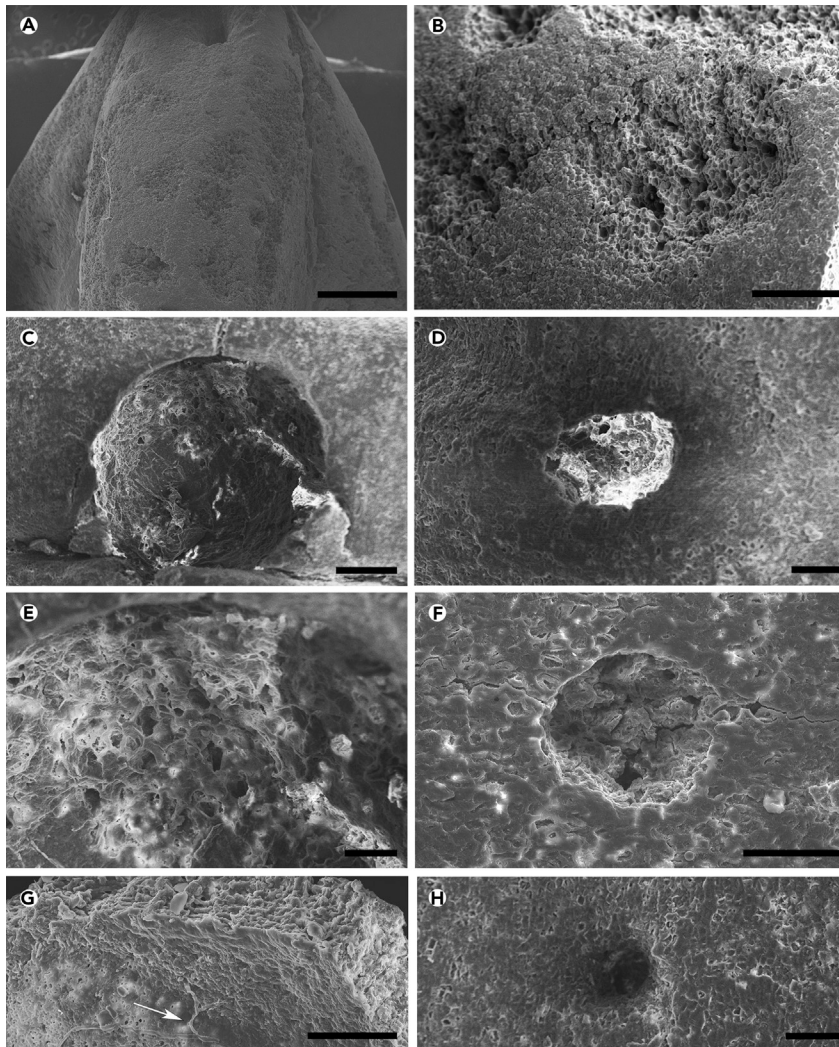
Figure 10. Damage on the pyrenes of *Canarium maomingense* sp. nov., SEM

(A) Shallow superficial damage of unknown nature, MMRH–196.

(B) Magnification of Figure 10A showing superficial damage.

(C) Fungal fruiting body, MMRH–213.

(D) Round hole, MMRH–213.

(E) Enlarged view of Figure 10C showing free hyphae and the body forming hyphae.

(F) Round hole, MMRH–213.

(G) Free hyphae on the endocarp surface (arrow), MMRH–213.

(H) Round hole, MMRH–213. Scale bars: (A) = 1 mm; (B and C) = 300 μm; (D–H) = 100 μm.

Limitations of the study

Most research studies of paleobotany are limited by materials of study. First, the number of plant macrofossil is limited. Secondly, the limitation of preservation of plant macrofossils. These two factors may affect the data representativeness, more accurate identification and classification based on morphology, and, eventually, reconstruction of paleogeography and paleoclimate.

STAR★METHODS

Detailed methods are provided in the online version of this paper and include the following:

- KEY RESOURCES TABLE
- RESOURCE AVAILABILITY

- ○ Lead contact
- ○ Materials availability
- ○ Data and code availability
- ● EXPERIMENTAL MODEL AND SUBJECT DETAILS
  - ○ Plants
- ● METHODS DETAILS
  - ○ Geological setting and terminology
  - ○ Specimens imaging and the nearest living relative method

SUPPLEMENTAL INFORMATION

Supplemental information can be found online at https://doi.org/10.1016/j.isci.2022.105385.

AUTHOR CONTRIBUTIONS

H.X., J.J., and X.W. conceived and designed the project. J.J., L.H., and X.W. organized field work and the collection of fossils. H.X. prepared, and imaged fossil and modern specimens, processed data. T.K., M.R., and N.M. interpreted the data on fossil fungi and participated in plate making. H.X., T.K., M.R., N.M., M.H., X.W., L.H., and J.J. contributed to initial manuscript preparation. All authors discussed results, read, revised, and approved the final manuscript.

DECLARATION OF INTERESTS

The authors declare there is no conflict of interest.

REFERENCES

1. Weeks, A., Daly, D.C., and Simpson, B.B. (2005). The phylogenetic history and biogeography of the frankincense and myrrh family (Burseraceae) based on nuclear and chloroplast sequence data. Mol. Phylogenet. Evol. 35, 85–101. https://doi.org/10.1016/j.ympev.2004.12.021.

2. Daly, D.C. (1989). Studies in neotropical Burseraceae. II. Generic limits in new world Protieae and Canarieae. Brittonia 41, 17–27.

3. Thulin, M., Beier, B.A., Razafimandimbison, S.G., and Banks, H.I. (2008). *Ambilobea*, a new genus from Madagascar, the position of *Aucoumea*, and comments on the tribal classification of the frankincense and myrrh family (Burseraceae). Nord. J. Bot. 26, 218–229. https://doi.org/10.1111/j.1756-1051.2008.00245.x.

4. Harley, M.M., Song, U., and Banks, H.I. (2005). Pollen morphology and systematics of Burseraceae. Grana 44, 282–299. https://doi.org/10.1080/00173130500477902.

5. Leenhouts, P.W. (1959). Revision of the Burseraceae of the Malaysian area in a wider sense. Xa. *Canarium* Stickm. Blumea 9, 275–475.

6. Weeks, A. (2009). Evolution of the pili nut genus (*Canarium* L., Burseraceae) and its cultivated species. Genet. Resour. Crop Evol. 56, 765–781. https://doi.org/10.1007/s10722-008-9400-4.

7. Peng, H., and Thulin, M. (2008). Burseraceae. In Flora of China, S.K. Chen, ed. (Science Press and Missouri Botanical Garden Press), pp. 106–110.

8. Vaughan, J.G. (1970). The Structure and Utilization of Oil Seeds (Chapman & Hall).

9. Wannan, B.S., and Quinn, C.J. (1990). Pericarp structure and generic affinities in the Anacardiaceae. Bot. J. Linn. Soc. 102, 225–252. https://doi.org/10.1111/j.1095-8339.1990.tb01878.x.

10. Plisko, M.A. (1996). Family anacardiaceae. In Comparative seed anatomy, 5, I. Rosidae and A.L. Takhtajan, eds. Dicotyledons (Mir I Semiya)), pp. 445–469. In Russian.

11. Bobrov, A.V.F.C., and Romanov, M.S. (2019). Morphogenesis of fruits and types of fruit of angiosperms. Bot. Lett. 166, 366–399. https://doi.org/10.1080/23818107.2019.1663448.

12. Han, M., Manchester, S.R., Wu, Y., Jin, J., and Quan, C. (2018). Fossil fruits of *Canarium* (Burseraceae) from Eastern Asia and their implications for phytogeographical history. J. Syst. Palaeontol. 16, 841–852. https://doi.org/10.1080/14772019.2017.1349624.

13. Tiffney, B.H. (1999). Fossil fruit and seed flora from the early Eocene Fisher/Sullivan site. In Early Eocene Vertebrates and plants from the Fisher/Sullivan site (Nanjemoy Formation) Stafford County, Virginia, R.E. Weems and G.J. Grimsley, eds. (Virginia Division of Mineral Resources)), pp. 139–159.

14. Tiffney, B.H., and Manchester, S.R. (2008). The Middle Eocene Wagon Bed Florule of Central Wyoming (U.S.A. Botanical Society of America). http://www.2008. botanyconference.org/engine/search/index. php?funcDdetail&aidD301.

15. Collinson, M.E., Manchester, S.R., and Wilde, V. (2012). Fossil fruits and seeds of the middle Eocene Messel biota, Germany. Abhandlungen der Senckenberg Gesellschaft für Naturforschung 570, 1–249.

16. Gregor, V.H.J., and Goth, K. (1979). First fossil record of the genus *Canarium* stickman 1759 (Burseraceae) in the European Paleogene. Stuttgarter Beiträge zur Naturkunde. Serie B (Geologie und Paläontologie) 47, 1–15. In German with English abstract.

17. Wing, S.L., and Tiffney, B.H. (1982). A Paleotropical Flora from the Jebel Qatrani Formation of Northern Egypt: APreliminary Report, 162 (Botanical Society of America, Miscellaneous Series Publication), p. 67.

18. Jacobs, B.F., Pan, A.D., and Scotese, C.R. (2010). A review of the cenozoic vegetation history of Africa. In Cenozoic Mammals of Africa, L. Werdelin and W.J. Sanders, eds. (University of California Press), pp. 57–72.

19. Kokawa, S. (1955). Plant and Insect Fossils Found in the Mikasayama Area, Nara Prefecture, 61 (The Geological Society of Japan), pp. 93–102, In Japanese with English abstract.

20. Yin, S.X., Wu, X.T., Wang, Z.X., and Shi, G.L. (2022). First fossil record of *Canarium* (Burseraceae) from the middle Miocene of Fujian, southeastern China and its paleoecological implications. Palaeoworld, in press. https://doi.org/10.1016/j.palwor.2022. 03.009.

21. Huang, L., Jin, J., and Oskolski, A.A. (2021). Mummified fossil of *Keteleeria* from the late Pleistocene of Maoming Basin, South China, and its phytogeographical and paleoecological implications. J. Syst. Evol. 59, 198–215. https://doi.org/10.1111/jse.12540.

22. Reid, E.M., and Chandler, M.E.J. (1933). The London Clay Flora (British Museum). Natural History.

23. Aggarwal, A., and Ambwani, K. (2000). *Canariocarpon ratnagiriensis* gen. et sp. nov. from Sindhudurg District, Maharashtra, India. J. Palaeosci. 49, 93–100.

24. N.J. Turland, J.H. Wiersema, F.R. Barrie, W. Greuter, D.L. Hawksworth, P.S. Herendeen, S. Knapp, W.H. Kusber, D.Z. Li, and K. Marhold, et al., eds (2018). International Code of Nomenclature for algae, fungi, and plants (Shenzhen Code) adopted by the Nineteenth International Botanical Congress Shenzhen, China, July 2017. Regnum Vegetabile 159 (Glashütten: Koeltz Botanical Books). https:// doi.org/10.12705/Code.2018.

25. Raven, P.H., and Axelrod, D.I. (1974). Angiosperm biogeography and past continental movements. Ann. Mo. Bot. Gard. 61, 539–673. https://doi.org/10.2307/ 2395021.

26. McLoughlin, S. (2001). The breakup history of Gondwana and its impact on pre-Cenozoic floristic provincialism. Aust. J. Bot. 49, 271–300. https://doi.org/10.1071/BT00023.

27. Lam, H.J. (1932). Beiträge zur morphologie der Burseraceae, insbesondere der Canarieae, 42 (Annales du Jardin Botanique de Buitenzorg.), pp. 97–226.

28. Renner, S.S., Clausing, G., and Meyer, K. (2001). Historical biogeography of Melastomataceae: the roles of Tertiary migration and long-distance dispersal. Am. J. Bot. 88, 1290–1300. https://doi.org/10.2307/ 3558340.

29. Davis, C.C., Fritsch, P.W., Bell, C.D., and Mathews, S. (2004). High latitude Tertiary migrations of an exclusively tropical clade: evidence from Malpighiaceae. Int. J. Plant Sci. 165, S107–S121. https://doi.org/10.1086/ 383337.

30. Weeks, A., Zapata, F., Pell, S.K., Daly, D.C., Mitchell, J.D., and Fine, P.V.A. (2014). To move or to evolve: contrasting patterns of intercontinental connectivity and climatic niche evolution in "Terebinthaceae" (Anacardiaceae and Burseraceae). Front. Genet. 5, 409. https://doi.org/10.3389/fgene. 2014.00409.

31. Li, S., Xing, Y., Valdes, P.J., Huang, Y., Su, T., Farnsworth, A., Lunt, D.J., Tang, H., Kennedy, A.T., and Zhou, Z. (2018). Oligocene climate signals and forcings in Eurasia revealed by plant macrofossil and modelling results. Gondwana Res. 61, 115–127. https://doi.org/ 10.1016/j.gr.2018.04.015.

32. Ling, C.C., Ma, F.J., Dong, J.L., Zhou, G.H., Wang, Q.J., and Sun, B.N. (2021). A mid-altitude area in southwestern China experienced a humid subtropical climate with subtle monsoon signatures during the early Oligocene: evidence from the Ningming flora of Guangxi. Palaeogeogr. Palaeoclimatol. Palaeoecol. 579, 110601. https://doi.org/10. 1016/j.palaeo.2021.110601.

33. Zachos, J.C., Shackleton, N.J., Revenaugh, J.S., Pälike, H., and Flower, B.P. (2001). Climate response to orbital forcing across the Oligocene–Miocene boundary. Science 292, 274–278. https://doi.org/10.1126/science. 1058288.

34. Westerhold, T., Marwan, N., Drury, A.J., Liebrand, D., Agnini, C., Anagnostou, E., Barnet, J.S.K., Bohaty, S.M., De Vleeschouwer, D., Florindo, F., et al. (2020). An astronomically dated record of Earth's climate and its predictability over the last 66 million years. Science 369, 1383–1387. https://doi.org/10.1126/science.aba6853.

35. Maloney, B.K. (1996). *Canarium* in the Southeast asian and oceanic archaeobotanical and pollen records. Antiquity 70, 926–933. https://doi.org/10. 1017/S0003598X00084180.

36. Premathilake, R., and Hunt, C.O. (2018). Late Pleistocene humans in Sri Lanka used plant resources: a phytolith record from Fahien rock shelter. Palaeogeogr. Palaeoclimatol. Palaeoecol. 505, 1–17. https://doi.org/10. 1016/j.palaeo.2018.05.015.

37. Lupo, K.D., Schmitt, D.N., Ndanga, J.P., Nguerede, L.P., Amaye, G.T., Smith, A.L., Edwards, N.M., Power, R.C., Craig Young, D., and Npo, F. (2021). Hunter-gatherers on the basin's edge: a preliminary look at Holocene human occupation of Nangara-Komba Shelter, Central African Republic. Azania 56, 4–33. https://doi.org/10.1080/0067270X. 2020.1865636.

38. Van Sam, H., Nanthavong, K., and Kessler, P.J.A. (2004). Trees of Laos and Vietnam: a field guide to 100 economically or ecologically important species. blum.J. Plant. Tax.Plant. Geog. 49, 201–349. https://doi. org/10.3767/000651904X484298.

39. Wei-dong, H., Xiu-mei, G., Lin-feng, L., and Chang-yi, L. (2001). Spatial pattern of dominant tree species of the secondary monsoon rain forest in Lianjiang, Guangdong Province. J. For. Res. 12, 101–104.

40. Do, D.S., and Nguyen, H.N. (2003). Use of Indigenous Tree Species in Reforestation in Vietnam (Agricultural Publishing House).

41. He, Z., and Xia, W. (2007). Nutritional composition of the kernels from *Canarium album* L. Food Chem. X. 102, 808–811. https://doi.org/10.1016/j.foodchem.2006. 06.017.

42. Huang, L.L., Jin, J.H., Quan, C., and Oskolski, A.A. (2021). New occurrences of Altingiaceae fossil woods from the Miocene and upper Pleistocene of South China with phytogeographic implications. J. Palaeogeogr. 10, 482–493. https://doi.org/ 10.1016/j.jop.2021.11.001.

43. Bazhenova, N.V., Wu, X.K., Kodrul, T.M., Maslova, N.P., Tekleva, M.V., Xu, S.L., and Jin, J.H. (2022). Mummified seed cones of *Pinus prehwangshanensis* sp. nov. (subgenus *Pinus*, Pinaceae) from the upper Pleistocene of Guangdong, South China: taxonomical significance and implication for phytogeography and ecology. Front. Ecol. Evol. 10, 900687. https://doi.org/10.3389/ fevo.2022.900687.

44. Ashton, P., and Zhu, H. (2020). The tropical-subtropical evergreen forest transition in East Asia: an exploration. Plant Divers. 42, 255–280. https://doi.org/10.1016/j.pld.2020. 04.001.

45. Köppen, W. (1936). Das geographische system der Klimate. In Handbuch der Klimatologie, W. Köppen and R. Geiger, eds. (Gebrüder Bornträger), pp. 1–44.

46. Peel, M.C., Finlayson, B.L., and McMahon, T.A. (2007). Updated world map of the Köppen–Geiger climate classification. Hydrol. Earth Syst. Sci. 11, 1633–1644. https:// doi.org/10.5194/hess-11-1633-2007.

47. Kannan, R. (1994). Burning out the black dammar, *Canarium strictum* Roxb. J. Bombay Nat. Hist. Soc. *91*, 159.

48. Banack, S.A. (1998). Diet selection and resource use by flying foxes (genus *Pteropus*). Ecology *79*, 1949–1967. https://doi.org/10.2307/176701.

49. Blate, G.M., Peart, D.R., and Leighton, M. (1998). Post-dispersal predation on isolated seeds: acomparative study of 40 tree species in a Southeast asian rainforest. Oikos *82*, 522–538.

50. Thomson, L.A., and Evans, J.B. (2006). *Canarium indicum* var. *indicum* and *C. harveyi* (canarium nut), ver. 2.1. In Species Profiles for Pacific Island Agroforestry, C.R. Elevitch, ed. (Permanent Agriculture Resources (PAR)). http://www.traditionaltree.org.

51. Almeida, F.C., Giannini, N.P., Simmons, N.B., and Helgen, K.M. (2014). Each flying fox on its own branch: a phylogenetic tree for *Pteropus* and related genera (Chiroptera: pteropodidae). Mol. Phylogenet. Evol. *77*, 83–95. https://doi.org/10.1016/j.ympev.2014.03.009.

52. May, B.M. (1993). Larvae of curculionoidea (insecta: Coleoptera): a systematic overview. Fauna N. Z. *28*. https://doi.org/10.7931/J2/FNZ.28.

53. Crous, P.W., Wingfield, M.J., Chooi, Y.H., Gilchrist, C.L.M., Lacey, E., Pitt, J.I., Roets, F., Swart, W.J., Cano-Lira, J.F., Valenzuela-Lopez, N., et al. (2020). Fungal Planet description sheets: 1042–1111. Persoonia *44*, 301–459. https://doi.org/10.3767/persoonia.2020.44.11.

54. Duka, I. (2015). Digicam control: free Windows DSLR camera controlling solution. http://digicamcontrol.com/.

55. Mosbrugger, V. (1999). The nearest living relative method. In Fossil plants and Spores: Modern Techniques, T.P. Jones and N.P. Rowe, eds. (Geological Society of London), pp. 261–265.

STAR★METHODS

KEY RESOURCES TABLE

REAGENT or RESOURCE	SOURCE	IDENTIFIER
Biological samples		
Canarium maomingense fossil specimens	Museum of Biology, Sun Yat-sen University, Guangzhou	MMRH–192; MMRH–193; MMRH–194; MMRH–195; MMRH–196; MMRH–197; MMRH–198; MMRH–207; MMRH–208; MMRH–209; MMRH–210; MMRH–211; MMRH–212; MMRH–213; MMRH–245; MMRH–246; MMRH–247
C. album	Museum of Biology, Sun Yat-sen University, Guangzhou	EC192247001
Software and algorithms		
Post-processing of images and color markings were performed with Adobe Photoshop 2020	Adobe Inc.	RRID: SCR_014199, URL: https://www.adobe.com/products/photoshop.html
DigiCamControl-Free Windows DSLR camera controlling solution	Duka, 2015	http://digicamcontrol.com/
Helicon Focus	Helicon Inc.	RRID:SCR_014462, URL: http://www.heliconsoft.com/heliconsoft-products/helicon-focus/
Dragonfly v.4.1	Comet Group	https://www.theobjects.com/dragonfly
GBIF	the Global Biodiversity Information Facility	RRID: SCR_005904, URL: https://doi.org/10.15468/dl.6nhprp
CUBG	ICCBG2022	https://image.cubg.cn/

RESOURCE AVAILABILITY

Lead contact

Further questions should be directed to the lead contact, Xinkai Wu (kakukaikai@163.com).

Materials availability

Fossil specimens MMRH–192, MMRH–193, MMRH–194, MMRH–195, MMRH–196 MMRH–197, MMRH–198, MMRH–207, MMRH–208, MMRH–209, MMRH–210, MMRH–211, MMRH–212, MMRH–213, MMRH–245, MMRH–246, MMRH–247, and extant *C. album* EC192247001 are deposited in the Museum of Biology, Sun Yat-sen University, Guangzhou, China. The comparison of *C. maomingense* with Asian extant *Canarium* species is available from Table S1. The comparison of *C. maomingense* with fossil species of *Canarium* and other related taxa is available from Table S2. Fossil records used in phytogeographic analyses is available from Table S3.

Data and code availability

- All data reported in this paper will be shared by the lead contact upon request.

- No novel code was used in this study.

- Any additional information required to reanalyze the data reported in this paper is available from the lead contact upon request.

EXPERIMENTAL MODEL AND SUBJECT DETAILS

Plants

All specimens used here were obtained from the source organizations listed in the key resources table.

METHODS DETAILS

Geological setting and terminology

The *Canarium* fossil fruits were collected from an opencast mine (21°52′47.5″N; 110°40′06.3″E) within the Maoming Basin, located near Zhenjiang Town, northwest of Maoming City, southwestern Guangdong Province, South China (Figure 1A). The fossiliferous deposits overlying with an angular unconformity the upper Eocene Huangniuling Formation have been dated to the late Pleistocene using accelerator mass spectrometry ^{14}C dating of fossil wood and fruit samples (28660 ± 140 and 26860 ± 130 BP, respectively), carried out at the Beta Analytic testing laboratory, Miami, Florida, USA.[21] The measured sedimentary succession with a total thickness about 2.5 m is composed of yellow sands with gravel and black, gray and grayish yellow mudstones (Figures 1B and 1C). Three-dimensionally preserved mummified fruits were obtained mainly from a layer of gray mudstone in the middle part of the studied succession. This sedimentary succession also includes conifers of the genera *Pinus* and *Keteleeria* (Pinaceae) and angiosperms belonging to *Elaeocarpus* (Elaeocarpaceae), *L. formosana* Hance (Altingiaceae), and Fagaceae.[21,42,43]

To describe the fruits of fossil and extant species of *Canarium*, carpological terminology was used based on those of previous studies.[5,9,11,27] The details of the fruit and pyrene anatomy of *Canarium* species are shown in Figure 2. The pyrene is treated as being composed of the inner zone of the mesocarp and the endocarp. The inner mesocarp zone is represented by thick-walled sclereids, while the innermost layer of the mesocarp is composed of relatively thin-walled cells, which separate the hard mesocarp tissue from the endocarp. Due to the decay of this layer of thin-walled cells, the endocarp may detach from the hard mesocarp tissue in fossil specimens. The endocarp is the innermost pericarp zone that develops from the locular (inner) epidermis and is represented in both studied extant and fossil species by one layer of stout palisade sclereids (*C. chandleri*, *C. indicum*, *C. luzonicum*) or by brachysclereids (*C. oleosum*).[8–11] The term "pyrene" is used in this study for identifying the inner hard fruit part instead of the term "endocarp", which is often applied to the hard tissues of the fossil fruits.

Specimens imaging and the nearest living relative method

Fossil fruits were cleaned with an ultrasonic cleaner (JieMeng JP–880) at a frequency of 42 kHz and photographed using a Nikon SMZ25 stereo microscope at the Museum of Biology, Sun Yat-sen University (Guangzhou, China). Extant fruits were photographed by a Canon EOS 760D digital camera. DigiCamControl-Free Windows DSLR camera controlling solution,[54] Helicon Focus 6.6.1 (Helicon Soft Ltd., Kharkov, Ukraine) and Photoshop 2020 (Adobe, San Jose, California, USA) were used for image processing. Microstructure was examined using a thermal field emission environmental scanning electron microscope (Quanta 400) at the test center, Sun Yat-sen University (Guangzhou, China). The internal three-dimensional structure of fruit was observed by Zeiss Xradia 520 Versa X-ray microscope (CT) housed at the University of Science and Technology of China (Hefei, China) and image data were processed using Dragonfly software.

The assumption that Cenozoic extinct plants and their nearest living relatives (NLRs) have similar environmental requirements, is the base of the NLR method. This method was used to estimate the paleoclimatic and paleoecologic conditions under which the studied fossil taxon lived by identifying the NLRs of fossil species and the environmental characteristics predominating in the regions of their modern natural distribution.[55]